GeoConvention
Calgary • Canada • March 7-11 2016
OPTIMIZING RESOURCES

Microseismic Quality Control Using Synthetic Seismograms

Sebastian D. Goodfellow, Junwei Huang, Edward Cottell, Mike Smith, Shawn C. Maxwell
Itasca Microseismic and Geomechanical Evaluation (IMaGE)

Summary

We describe a method for rapid generation of synthetic waveforms to aid in quality control analysis of microseismic data. The method utilizes two-point ray tracing to calculate the travel time, ray distance, source vector of direct waves, critical refracted waves, and reflected waves. This information is then used to generate synthetic waveforms by placing a series of user defined wavelets at the arrival time of each phase. The amplitude of each wavelet was then corrected to account for geometric spreading, anelastic attenuation, reflection and transmission losses, and source radation pattern. Lastly, the output from our ray synthetic function was compared with the more computationally intense full waveform solution using such as Finite Difference and Finite Element methods and showed good agreement.

We demonstrate the effectiveness of this technology on real microseismic data from a downhole hydraulic fracture operation. The ray synthetics allowed for better understanding of complex waveforms leading to more accurate phase identification and improve source location confidence. The synthetics can also be used to correlation different processing results with the observed signals to quantify which results best match the recorded signals. Such an analysis can avoid the commonly reported pitfall of having different results from different processors and not knowing which to believe.

Introduction

Synthetic microseismic waveforms wave been used to test microseismic hypocenter location procedures within hypothetical but realistic geological structures and receiver array configurations (Tian and Chen, 2005) but are not used during routine analysis of microseismic data. Potential applications in microseismic data processing include algorithm validation, model calibration, waveform prediction, acquisition optimization, and source mechanism evaluation. Given the vast potential uses of synthetic waveforms, we propose a ray-based method to generate accurate synthetic waveforms in a timely manner. Comparing with full waveform solution, this method saves significant amount of time in model preparation and waveform simulation and still preserve the primary seismic phases in the full waveform seismograms.

Theory and Method

Ray tracing for synthetic generation is conducted using the two-point formulation of Tian and Chen, 2005 (Tian Ray Tracing Method). The Tian method minimizes the following function,

$$F(q) = q\sum_{k=1}^{l} \frac{\varepsilon_k \tilde{h}_k}{\sqrt{\tilde{h}_M^2 + \left(1-\varepsilon_k^2\right)q^2}} - \Delta_0 , \qquad (1)$$

where h_M is the effective height of the fastest layer, h_k is the effective height of the k^{th} layer and Δ_0 is the given epicentral distance between the source a receiver. Refer to Tian and Chen, 2005 for more details.

Synthetic waveforms include contributions from direct waves, refracted waves and reflected waves. For reflected waves, this only includes the primary reflection on each layer above and below the source, as multiple reflections are not easily identified in field data. Figure 1 shows a ray tracing example

for each wave type. The velocity model was taken from the work of Wong et al., 2015 and was modelled after the geological structure typically encountered in the Barnett shale.

A synthetics waveform is generated by first placing a user defined pulse shaped wavelet at the arrival time of all direct waves and all possible refracted waves and reflected waves. For example, the $\sin^3$ source function is presented in equation 2,

$$f''(t) = 4\sin^3\left(\frac{\pi t}{T}\right)\cos\left(\frac{\pi t}{T}\right), \tag{2}$$

where T controls the pulse width. Other wavelets such as Ricker, Ormsby, Klauder, etc. can be used as well (Ryan, 1994),

The amplitude of each wavelet was corrected for geometric spreading, anelastic attenuation and losses due to impedance contrasts at layer boundaries using plane wave reflection and transition coefficients (Aki and Richards, 1980). We also included amplitude variations to model the source radiation pattern (Aki and Richards, 1980) for a double-couple source mechanism defined by the strike and dip of the fracture plane, and the rake, the slip direction. Figure 2 presents an example (same velocity model as Figure 1) showing the ray synthetic output for a double-couple source with strike = 0^0, dip = 45^0, and rake = 90^0. The synthetics waveforms include all direct, refracted and reflected waves, where the reflected wave arrival times are indicated by red ticks instead of wavelets to reduce the complexity of the waveforms so that the radiation pattern effect could be clearly demonstrated.

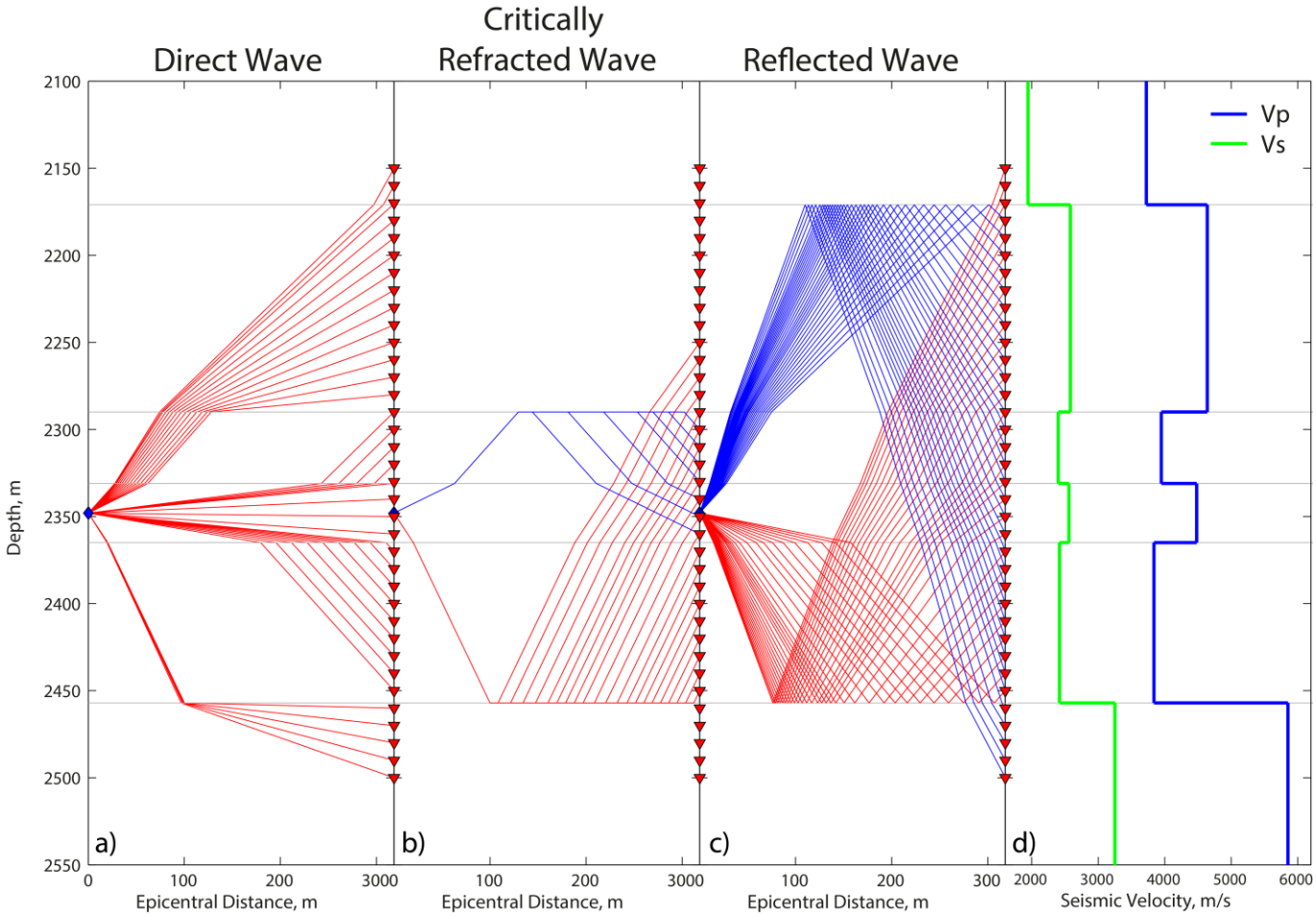

Figure 1: Ray tracing example, a) direct wave, b) critically refracted wave, c) reflected wave, d) velocity model.

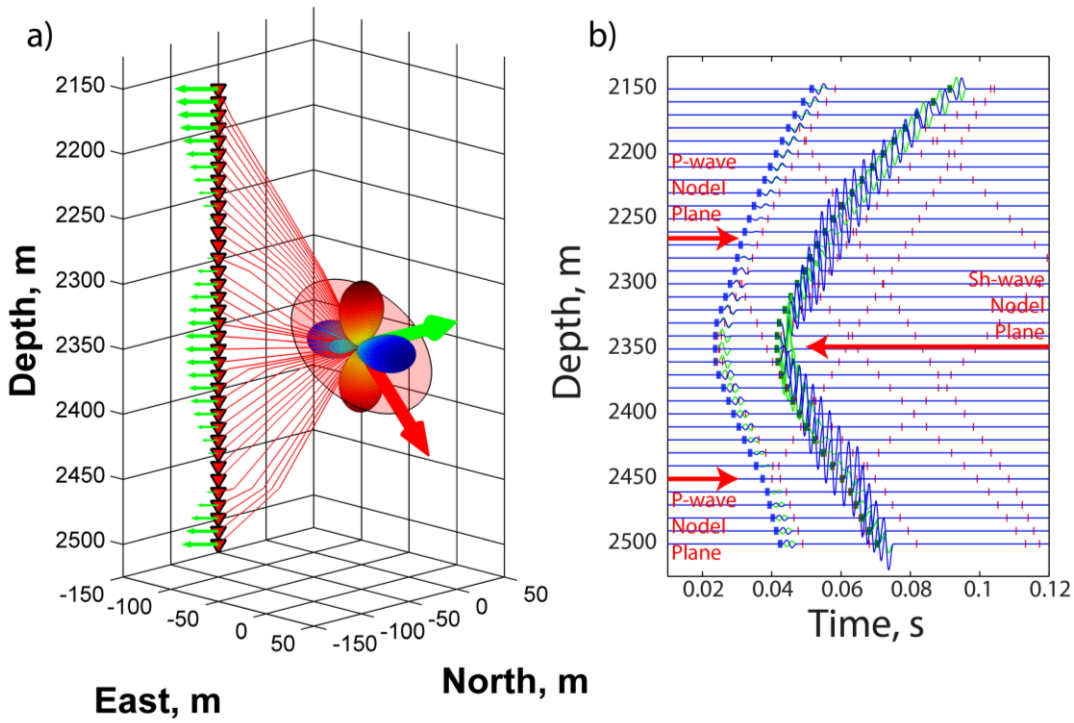

Figure 2: Ray synthetic example, a) array geometry, direct P-wave ray trajectories, P-wave radiation pattern, b) ray-based synthetic waveforms captures the main features including the primary reflection, amplitude attenuation, and nodal plane.

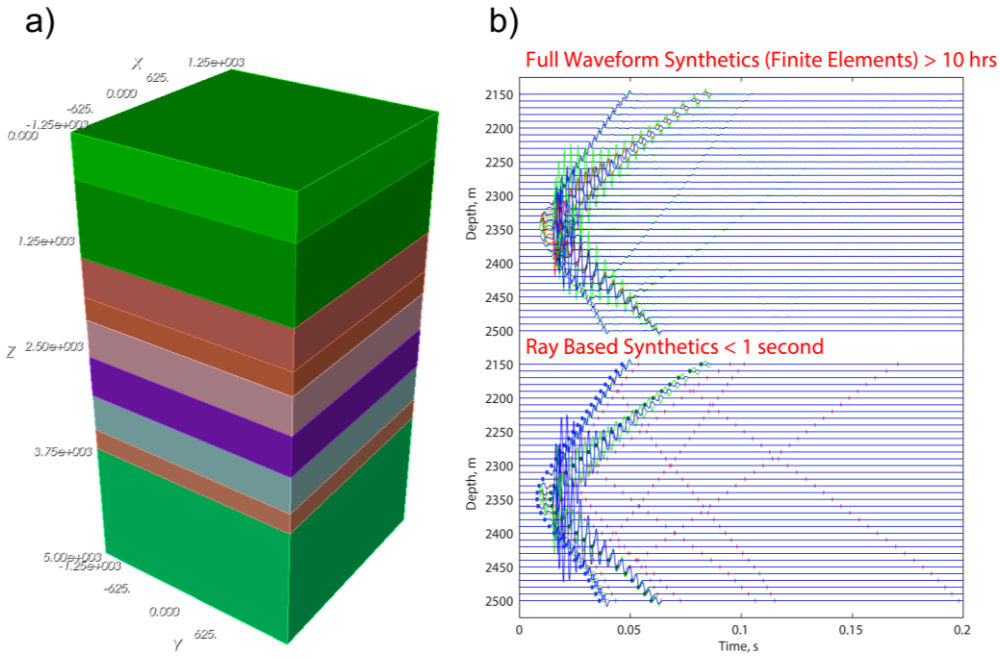

Figure 3: Comparison with full waveform modelling, a) a 3D layered model with each layer distinguished by a different color, b) synthetic waveforms using ray synthetics method and full waveform method.

Each receiver ray vector is decomposed into the sensor local coordinates (X, Y, and Z axes) and can then be automatically rotated to a North, East, Down or P, Sh, Sv coordinate system.

Next, the ray synthetic waveforms were compared with synthetic waveforms using spectral finite element method (Komatitsch and Tromp, 1999) to verify the accuracy of this method. An example of the 3D layered model, a snapshot of the full wave field and a waveform comparison is presented in Figure 3. Both synthetics were generated using the same source mechanism (strike = 0^0, dip = 45^0, and rake = 90^0) and show good agreement. The seismic phases commonly used in microseismic monitoring, i.e., the direct and refracted arrivals (marked by blue lines in Figure 4), are reproduced with high accuracy and other phases not used in microseismic processing are excluded. As a comparison, a 2D slice from a 3D full wave field presented in Figure 4 show the complexity of the wave field even in a simple layered isotropic model. The secondary phases such as multiple reflections that are not used in microseismic processing consumes extra computation resources and complicate the waveform analysis.

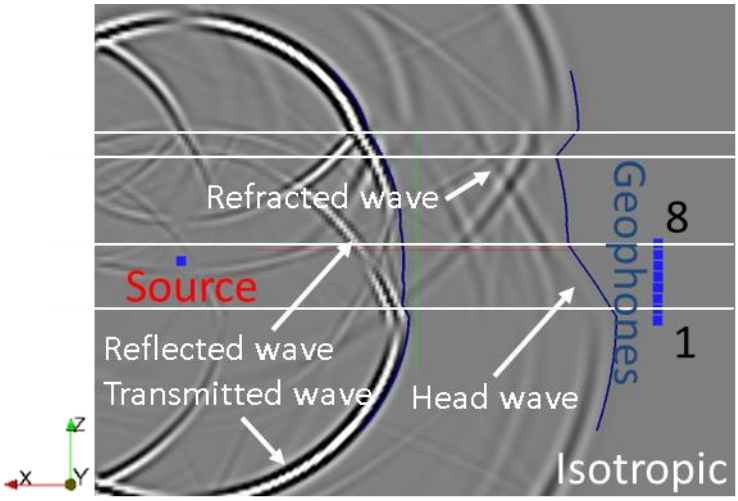

Figure 4: One snapshot of the full waveform field shows the complexity of the wave field even in a simple 1D isotropic model. Secondary phases such as multiple reflections that are not commonly used in microseismic processing are present and complicate the waveform analysis.

Conclusions

In this paper, we have presented an effective technique in generating controlled seismic waveform based on two-point ray tracing. Comparing with full waveform solution, our method is efficient in CPU time and is able to reserve the seismic phases that are used in microseismic data processing and quality control. In addition, the user defined seismic source radiation pattern is built in the fracture plane based discontinous source model. The full physics controlling the amplitude have been account for such as geometrical spreading, anelastic attenuation, and transmission and reflection losses. The synthetics can be used to correlate different processing results with the observed signals to quantify which results best match the recorded signals and avoid the pitfalls of having different results from different processors.

Acknowledgements

We thank the members of staff at IMaGE for their support in this work.

References

Aki, K., and Richards, P., 1980, *Quantitative Seismology: Theory and Methods*, W. H. Freeman, New York.

Komatitsch, D. and Tromp J., 1999, Introduction to the spectral-element method for 3-D seismic wave propagation, Geophysical Journal International, vol. 139, p. 806-822.

Ryan, H., 1994, Ricker, Ormsby, Klander, Butterworth - A Choice of wavelets, Vol 19, Issue 7, Pages 8-9.

Tian Y., and Chen X-F., 2005, A rapid and accurate two-point ray tracing method in horizontally layered velocity model: Acta Seismologica Sinica, 18, 154 – 161.

Wong, J., Manning, P. M., Han, L., and Bancroft, J. C., 2015, Synthetic Microseismic Datasets: CSEG Recorder, 36.